SUPPLEMENT TO THE *WELDING JOURNAL*, SEPTEMBER 2005
Sponsored by the American Welding Society and the Welding Research Council

Influence of Procedure Variables on C-Mn-Ni-Mo Metal Cored Wire Ferritic All-Weld Metal

Welding position, number of layers, arc energy, and shielding gas type were considered

BY N. M. RAMINI DE RISSONE, H. G. SVOBODA, E. S. SURIAN, AND L. A. DE VEDIA

ABSTRACT. The objective of this work was to study the effects that the utilization of different shielding gases (CO_2 and a 80% Ar/20% CO_2 mixture), welding position (flat and uphill), arc energy and number of passes per layer (two and three) have on the all-weld-metal microstructure and mechanical properties from an ANSI/AWS A5.29-98 E91T5-K2/E101T5-K3 metal cored wire, 1.2 mm diameter. Hardness, tensile, and impact tests were used to assess the mechanical properties, and quantitative metallographic analyses were performed to identify the resulting microstructures. ANSI/AWS A5.29-98 E91T5-K2 tensile property requirements were satisfied under Ar/CO_2 shielding and the E101T5-K3 chemical composition specification was met in all conditions. E91T5-K2/E101T5-K3 toughness requirements were comfortably satisfied under both gas types, but significant variations were found with different welding procedures. These variations have been rationalized in terms of the microstructure and chemical composition of the weld deposits. The results obtained in this work showed that, as in the case of SMAW electrodes of the type ANSI/AWS A5.5-96 E10018/11018/12018-M types, depositing C-Mn-Ni-Mo or C-Mn-Ni-Mo-Cr alloyed ferritic weld metal, the main difficulty resides in obtaining adequate tensile strength values rather than in satisfying toughness requirements that can be obtained almost in any welding condition, within the requirements of the appropriate standard.

N. M. RAMINI DE RISSONE is with DEYTEMA – Technology of Materials Research Center, Regional Faculty San Nicolás, National Technological University, San Nicolás, Argentina. H. G. SVOBODA is with Metallurgy Laboratory, Naval and Mechanical Engineering Department, Faculty of Engineering, University of Buenos Aires, Buenos Aires, Argentina. E. S. SURIAN is Research Secretary, Faculty of Engineering, National University of Lomas de Zamora, Buenos Aires, Argentina/DEYTEMA – Technology of Materials Research Center, Regional Faculty San Nicolás, National Technological University, San Nicolás, Argentina. L. A. DE VEDIA is with Institute of Technology Prof. Jorge A. Sabato, National University of San Martín, National Atomic Energy Commission, CIC, Buenos Aires, Argentina.

Introduction

During the last 20 to 30 years, there has been a worldwide trend toward replacing covered electrodes for manual welding with other processes that allow a higher deposition rate and lend themselves better for automation (Ref. 1). In spite of the fact that because of some particular features of the shielded metal arc welding process (Ref. 2), it will not be completely replaced in the foreseeable future, and it is estimated that around 70% of the deposited weld metal will come from more efficient processes. Continuous wires are increasingly used, among them flux and metal cored wires that, due to the versatility of these welding consumables, can be produced in relatively small quantities of electrodes of a wide variety of weld deposits with different chemical compositions and which exhibit adequate mechanical properties for all-position welding (Refs. 3–5).

Among the different cored wire types, those used under gas protection can be classified as flux cored and metal cored wires. They present different characteristics, advantages, and disadvantages. It is known that flux cored wires provide improved joint penetration, smooth arc transfer, low spatter level, and most important, are easier to use than solid wires (Refs. 6, 7); with them it is also possible to achieve high deposition rates (Refs. 6, 7). Metal cored wires present an important technological advantage due to the near absence of slag, which makes them adequate for robotic welding (Refs. 6, 8).

On the other hand, it is well known that the employment of different shielding gases, as well as changes in welding procedure parameters, lead to variations in the deposit characteristics (Refs. 9–17). Generally, the most frequently used gas for welding with rutile-type flux cored wires is CO_2, but it is also possible to use Ar/CO_2 mixtures. This type of protection results in improved appearance, less spatter, and better arc stability (Ref. 9). On the other hand, in all arc welding processes, it is important that the arc energy control influence metallurgical transformations and resulting mechanical properties and microstructure (Refs. 10–14). In multipass welding, changes in welding parameters lead to different arc energies and different number of passes per layer for the same joint design (Refs. 10, 11). Welding position is another important variable (Ref. 16).

In particular, the objective of this work was to study the effect of shielding gas type (CO_2 and Ar/CO_2 mixture), flat and uphill welding positions, arc energy (between 1.2 and 2.2 kJ/mm), and number of passes per layer (2 and 3) on the all-weld-metal mechanical properties and microstructure, obtained from a metal cored wire, of the ANSI/AWS A5.29-98 E91T5K2/E101T5-K3 type.

KEYWORDS

Metal Cored Wire
Shielding Gas
Ferritic All-Weld-Metal
Flat Position
Uphill Position
Charpy V-Notch Test

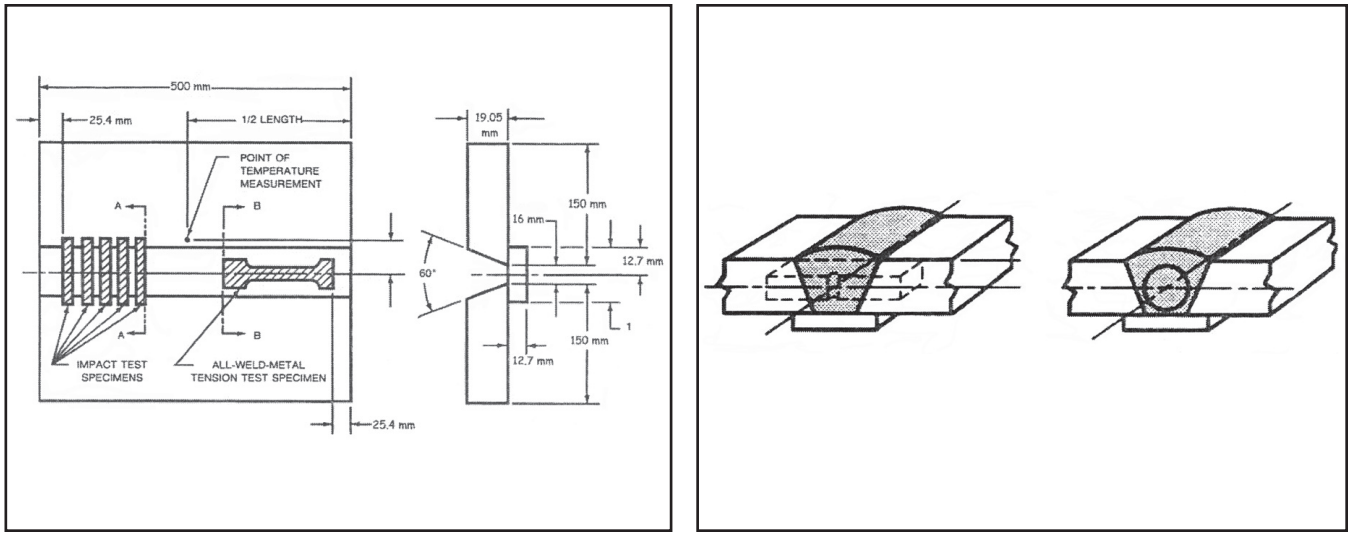

Fig. 1 — A — Location of test specimens in plan view (left) and cross section showing joint preparation (right); B — location of impact (left) and tensile (right) test specimens in perspective.

Table 1 — Test Specimen Identification and Welding Parameters Used

Sample	Welding position	Shielding gas	Number of passes	Number of layers	Current (A)	Voltage (V)	Welding speed (mm/s)	Heat input (kJ/mm)
C2F	Flat	CO_2	2	6	238	29	3.6	2.0
C3F	Flat	CO_2	3	6	193	26	4.1	1.5
A2F	Flat	Ar/CO_2	2	6	234	28	3.4	2.2
A3F	Flat	Ar/CO_2	3	6	197	25	4.6	1.2
C2V	Uphill	CO_2	2	6	145	20	1.7	1.8
C3V	Uphill	CO_2	3	6	135	18	2.3	1.3
A2V	Uphill	Ar/CO_2	2	6	160	19	2	1.6
A3V	Uphill	Ar/CO_2	3	6	149	18	2.6	1.2
AWS req.*			2 or 3	5 to 8	NS	NS	NS	NS

*only for flat welding position.
Preheating temperature was 150°C. Interpass temperature was in the range 140–150°C. The plates were buttered with the same electrode used as filler and preset to avoid restraining. Electrode extension was 20 mm in all cases. Gas flow in both cases: 20 L/min. NS: not specified.

Experimental Procedure

Weldments

Electrodes

The consumable employed in this work was a commercial product classified by the fabricator as ANSI/AWS A5.29-98 (Ref. 18) E91T5-K3 type metal cored wire, in 1.2 mm diameter. In fact, according to the mentioned standard, there are two classifications: E91T5-K2 and E101T5-K3. It is supposed that the fabricator made an extrapolation taking into account the all-weld metal both in terms of chemical composition and mechanical properties of the consumable.

Test Specimens

With this wire, eight all-weld-metal

Table 2 — All-Weld-Metal Chemical Composition (all the elements in wt-% except N and O, which are in ppm).

Sample	C2F	C3F	A2F	A3F	C2V	C3V	A2V	A3V	AWS req. E91T5-K2	AWS req. E101T5-K3
C	0.043	0.035	0.063	0.048	0.070	0.074	0.079	0.081	0.15 max.	0.15 max.
Si	0.31	0.27	0.40	0.43	0.36	0.34	0.43	0.46	0.80 max.	0.80 max.
Mn	1.26	1.14	1.43	1.47	1.38	1.36	1.56	1.55	0.50–1.75	0.75–2.25
P	0.010	0.010	0.010	0.009	0.010	0.010	0.010	0.011	0.03 max.	0.03 max.
S	0.009	0.009	0.009	0.009	0.009	0.009	0.009	0.009	0.03 max.	0.03 max.
Cr	0.04	0.04	0.04	0.04	0.04	0.04	0.04	0.04	0.15 max.	0.15 max.
Mo	0.45	0.45	0.42	0.44	0.41	0.43	0.41	0.42	0.35 max.	0.25–0.65
Ni	1.86	1.90	1.79	1.79	1.82	1.85	1.90	1.92	1.0–2.0	1.25–2.60
Al	<0.01	<0.01	<0.01	<0.01	<0.01	<0.01	<0.01	<0.01	NS	NS
Co	0.04	0.04	0.04	0.04	0.04	0.04	0.04	0.04	NS	NS
Cu	0.04	0.03	0.04	0.03	0.03	0.03	0.03	0.03	NS	NS
V	0.01	0.01	0.01	0.01	0.01	0.01	0.01	0.01	NS	NS
N (ppm)	31	28	40	26	27	29	23	27	NS	NS
O (ppm)	693	755	558	573	706	724	598	561	NS	NS
Heat input (kJ/mm)	2.0	1.5	2.2	1.2	1.8	1.3	1.6	1.2	NS	NS

test coupons were made with the weld preparation for the flat welding position of the ANSI/AWS A5.29-98 standard (Ref. 18), which is shown in Fig. 1A, using the following:

- Two shielding gases: pure CO_2 and a mixture of 80% Ar–20% CO_2 (Ar/CO_2)
- Two arc energies: high (two beads per layer) and low (three beads per layer)
- Flat and uphill welding positions.

The key to the identification of the weld test specimens is as follows: C means welding under CO_2 and A welding under Ar/CO_2 shielding; 2 or 3 represent the number of passes per layer; while F and V are the flat and uphill welding positions, respectively. The welding parameters employed are shown in Table 1.

Tensile Tests, Impact Tests, and Hardness Measurements

From each all-weld-metal test coupon, a Minitrac (Ref. 19) tensile specimen (total length = 55 mm, gauge length = 25 mm, reduced section diameter = 5 mm, gauge length-to-diameter ratio = 5:1) and enough Charpy-V specimens with the notch located as shown in Fig. 1B, to construct the absorbed energy vs. test temperature curve between –80° and 20°C, were machined. A cross section was also obtained from each specimen to conduct both a microhardness survey, at the Charpy V-notch location, using a 1000-g load and the metallographic analysis. Tensile tests and Charpy-V impact tests were performed in the as-welded condition. Prior to testing at room temperature, tensile specimens were heat treated for 24 h at 200°C (328°F) to let hydrogen diffuse away.

Chemical Composition

All-weld-metal spectrometric chemical analyses were conducted on a cross section of each weld coupon. Nitrogen and oxygen determinations were made with LECO equipment extracting the samples from the broken ends of the tensile specimens.

Metallographic Study

Examination of cross sections (etched with 2% Nital) was carried out in the top beads and in the Charpy V-notch location (Fig. 2), as described previously (Ref. 20). The area fractions of columnar and reheated zones were measured at 500x at the Charpy V-notch location. The average width of the columnar grain size (prior austenite grains) was measured in the top bead of the samples, at 100x. To quantify the microstructural constituents of the columnar zones, in each weld, 10 fields of 100 points were measured, in the top bead, at 500x by light microscopy.

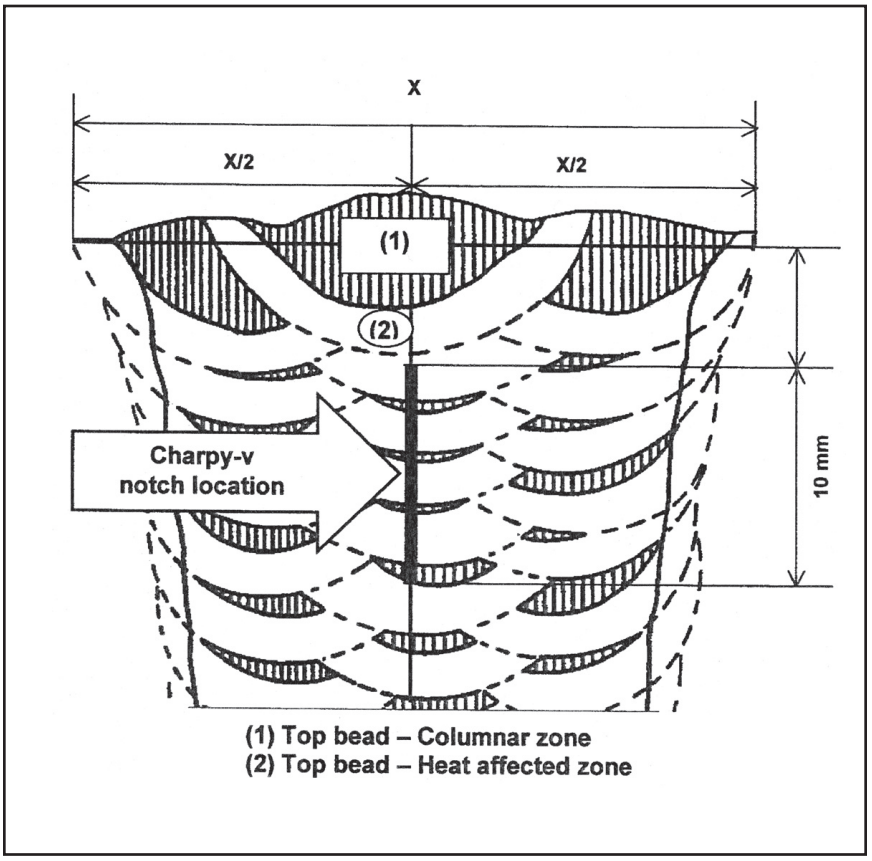

Fig. 2 — Cross section of the all-weld-metal test assembly.

Results and Discussion

All-Weld-Metal Chemical Composition

Table 2 presents the all-weld-metal chemical composition obtained from the mechanical property test coupons.

A marked variation in the oxygen levels was observed; higher values corresponding to welds made with CO_2 shielding. Due to this difference, carbon, manganese, and silicon values were lower for this gas. It has been shown (Ref. 5) that when using an Ar/CO_2 gas mixture instead of pure CO_2 for the same wire, the O content in the gas mixture, originated from the decomposition of CO_2 decreases, and also the O partial pressure in the arc. A smaller amount of Mn and Si will be oxidized under Ar/CO_2 than under CO_2, leading to a higher recovery of these elements in the weld metal. Mo and Ni contents were insensitive to the O variations.

Table 3 — Vickers Hardness Measurements and Percentages of Both Columnar and Fine and Coarse Grain Heat-Affected Zones, Corresponding to the Charpy V-Notch Location

Sample	C2F	C3F	A2F	A3F	C2V	C3V	A2V	A3V
VH*	221	219	239	248	243	263	263	278
% CG-HAZ	20	22	27	14	10	23	13	13
% FG-HAZ	26	22	22	15	12	18	13	11
%HAZ	46	44	49	29	22	41	26	24
%CZ	54	56	51	71	78	59	74	76
Heat input (kJ/mm)	2.0	1.5	2.2	1.2	1.8	1.3	1.6	1.2

VH*: Vickers hardness; CG: coarse grain; FG: fine grain; HAZ: heat-affected zone; CZ: columnar zone.

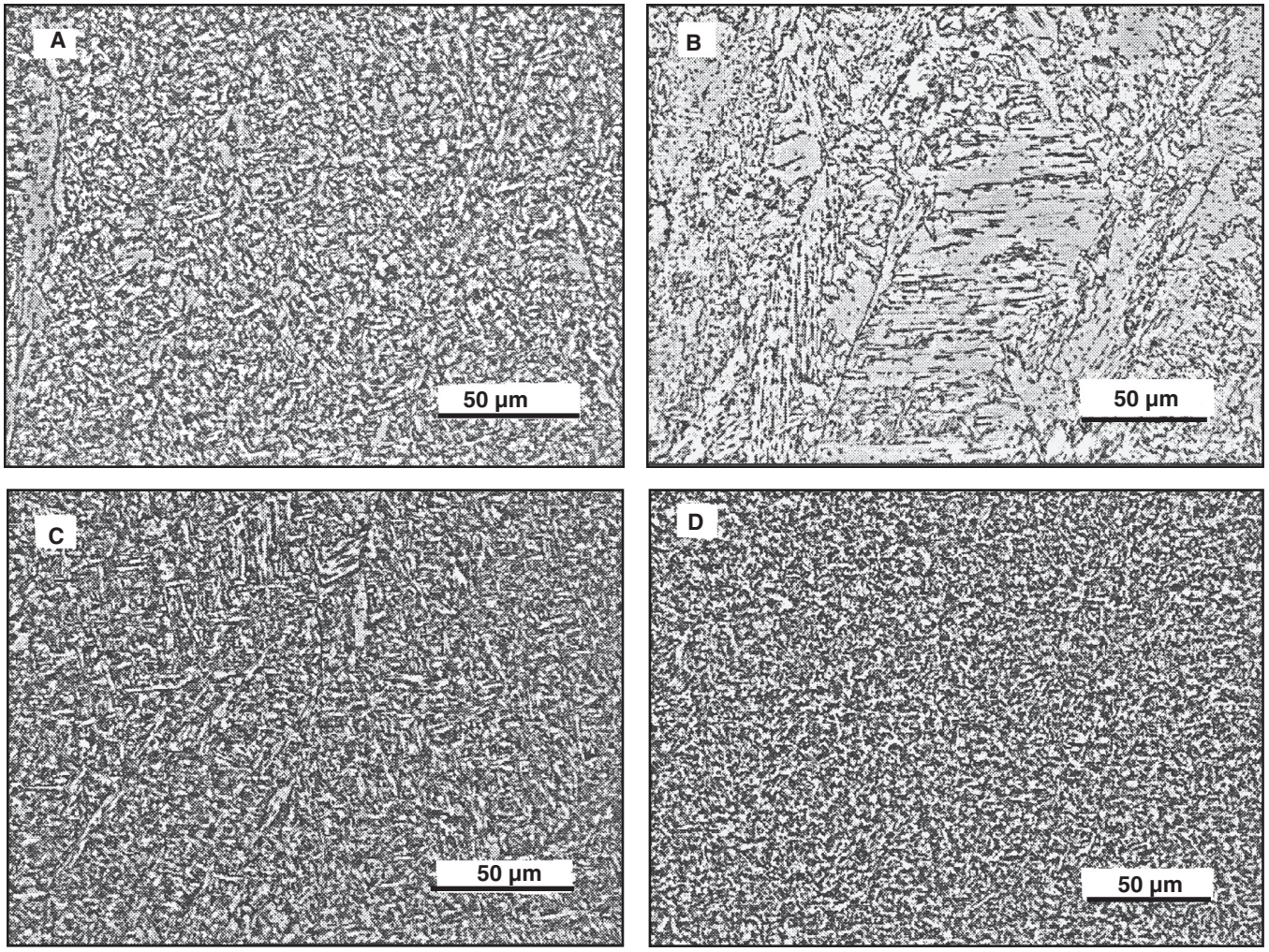

Fig. 3 — Last bead columnar zones; A — Weld A2F; B — weld C3F; C — weld A2V; D — weld C3V.

Table 4 — Top Bead Columnar Zone Microconstituents and Prior Austenite Grain Width

Sample	Heat input (kJ/mm)	AF%	PF(G)%	PF(I)%	FS(NA)%	FS(A)%	FS %	PAGW (mm)
C2F	2.0	15	22	7	53	3	56	107
C3F	1.5	7	36	5	37	15	52	97
A2F	2.2	45	13	12	28	2	30	120
A3F	1.2	37	12	14	31	6	37	103
C2V	1.8	25	5	15	52	3	55	—
C3V	1.3	16	0	16	66	2	68	—
A2V	1.6	42	4	19	33	2	35	—
A3V	1.2	32	2	13	48	5	53	—

AF: acicular ferrite; PF(G): grain boundary ferrite; PF: polygonal ferrite; FS(NA): ferrite with second phase not aligned; FS(A): ferrite with second phase aligned; FS: ferrite with second phase; PAGW: prior austenite grain width.

Nitrogen values were very low, as well as residual elements of P, S, Cr, V, Co, Cu, and Al, showing a very clean weld deposit. No influence of the heat input (two or three passes per layer) was detected on the chemical composition, but the C, Mn, and Si values were somewhat lower in the welds obtained in flat welding positions than in uphill, as was previously found (Refs. 16, 21, 22).

Considering chemical composition under both gas protections, only the ANSI/AWS A5.29-98 E101T5-K3 requirements were satisfied. The all-weld-metal Mo content exceeded the maximum value required by the E91T5-K2 classification.

Metallographic Analysis

General

Table 3 shows the percentages of columnar and reheated zones corresponding to the Charpy V-notch location. As a general tendency, it was seen that the proportion of columnar zones was larger in samples welded with lower arc energy, 3 passes per layer, as previously found (Refs. 10, 11, 21–23). This fact would be mainly related to the geometrical distribution of the weld beads with respect to the location of the Charpy-V specimen notch and to the increase in columnar zone proportion against the reheated zone area when the heat input is reduced as found by Evans (Ref. 23). In samples C2V and C3V, a different behavior was detected; the proportion of columnar zones was larger in samples welded with higher arc energy,

two passes per layer. This was probably due to the difficulties found during microstructural assessment given the little morphological differences between different zones in these samples. This fact is compounded with the intrinsic characteristics of uphill welds, which result in lower current, arc voltage, and welding speed (increased weaving) for the same heat input, which gives rise to a different bead shape than in the flat position.

Columnar Zone (As Welded)

Table 4 shows the percentages of microconstituents present in the columnar zone of the last bead of each weld.

For samples welded in the flat position, the percentages of grain boundary primary ferrite [PF(G)] and ferrite with second phase, aligned [FS(A)] and not aligned [FS(NA)], decreased and acicular ferrite [AF] and intragranular primary ferrite [PF(I)] increased, when using the gas mixture, compared to those welded under CO_2 shielding — Fig. 3A (A2F) and 3B (C3F). A correlation between microstructural development and weld metal chemi-

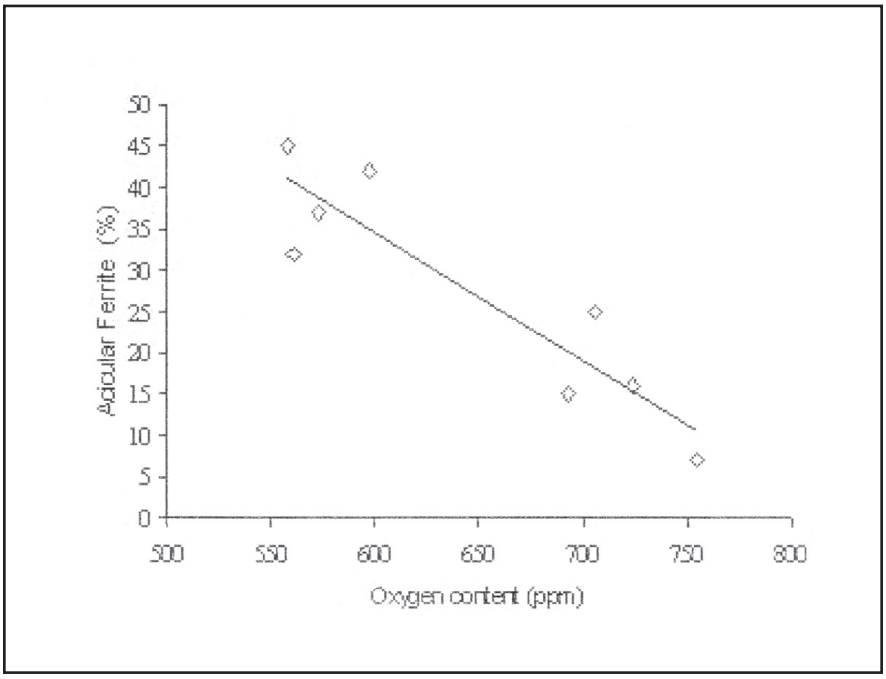

Fig. 4 — Oxygen contents vs. AF percentages.

Table 5 — All-Weld-Metal Tensile Property Test Results

Property	C2F	C3F	A2F	A3F	C2V	C3V	A2V	A3V	E91T5-K2	E101T5-K3
TS (MPa)	661	625	699	699	724	724	771	766	620–760	690–830
YS (MPa)	492	502	503	587	536	625	645	646	540 min	610 min
E (%)	28	20	20	21	18	20	21	20	17 min	16 min
Heat input (kJ/mm)	2.0	1.5	2.2	1.2	1.8	1.3	1.6	1.2	NS	NS

TS: tensile strength; YS: yield strength; E: elongation; NS: not specified.

Table 6 — Record of Charpy-V Impact Test Values in J

(°C)	C2F	C3F	A2F	A3F	C2V	C3V	A2V	A3V
20	120-106-118	113-108-112	123-134-129	146-114-116	116-116-122	98-102-95	114-119-106	108-104-98
	115	111	129	125	118	98	113	103
0	114-115-120	87-97-100	116-126-119	122-128-112	116-118-114	86-97-90	108-109-109	97-103-88
	116	95	120	121	116	91	109	96
–20	110-106-97	72-80-73	120-117-112	98-105-112	106-99-107	67-57-69	96-101-107	77-93-75
	104	75	116	105	104	64	101	82
–40	76-90-64	69-47-48	104-109-93	68-57-59	103-97-91	61-57-57	89-83-83	79-77-68
	77	55	102	61	97	58	85	75
–60	85-67-50	36-39-47	66-64-68	79-47-58	71-79-74	44-46-38	68-78-68	45-56-57
	67	41	66	61	75	43	71	53
–80	28-41-20	37-27-27	31-36-29	47-63-61	53-48-73	51-49-49	64-57-52	61-62-72
	30	30	32	57	58	50	58	65

ANSI/AWS E91T5-K2/E101T5-K3 Charpy-V requirements are on average 27 J at –51°C. Figures in the upper line are measured values; figures in the lower line are averages.

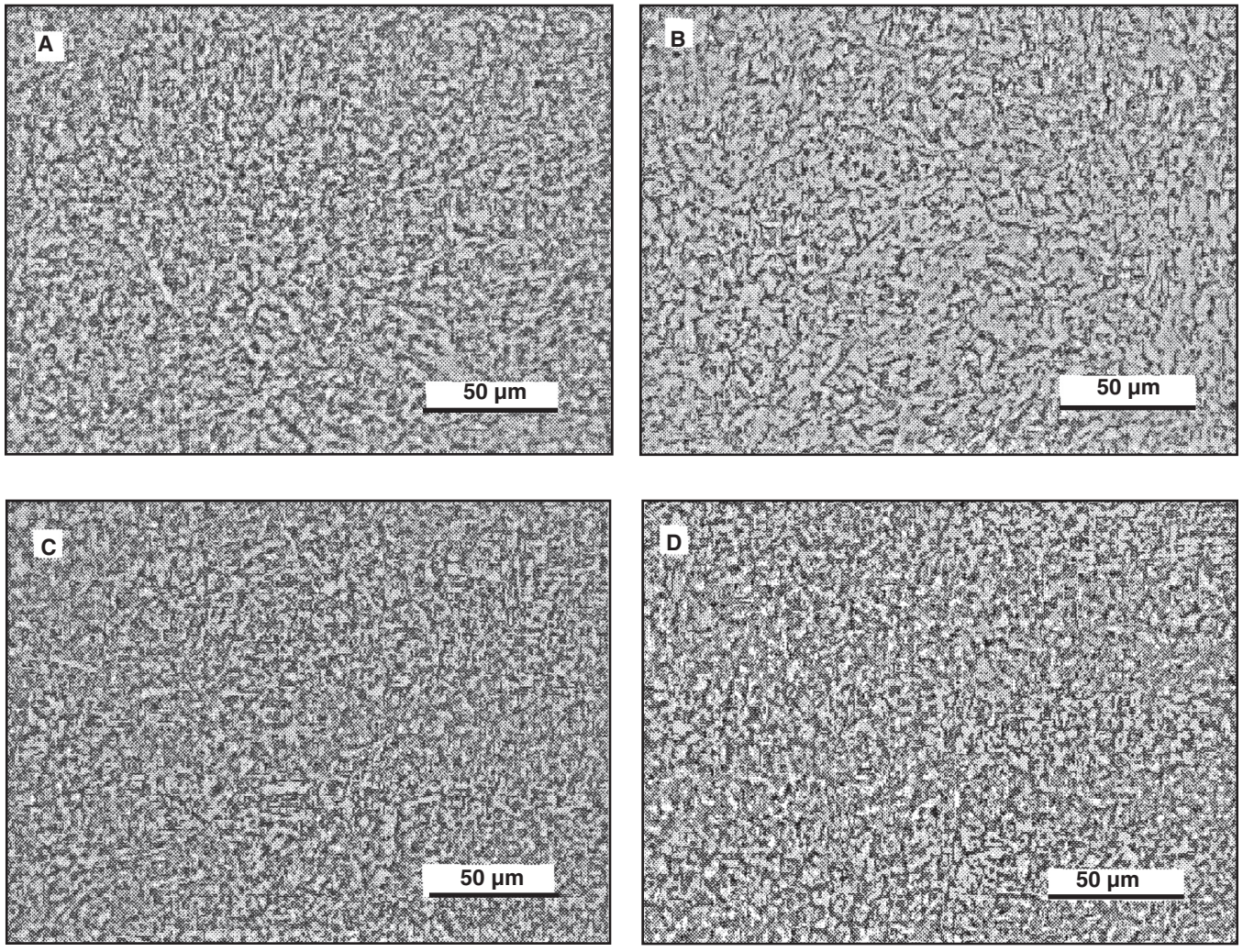

Fig. 5 — Last bead reheated zones; A — Weld A2F; B — weld C3F; C — weld A2V; and D — weld C3V.

cal composition can be observed. Weld C3F with the lowest C, Mn, and Si, and highest O contents, showed the smallest amount of AF and the highest proportion of PF(G), while weld A2F with the highest values of C, Mn, and Si, and the lowest O content, exhibited the highest proportion of AF and the lowest content of PF(G).

The lower C, Mn, and Si contents in the test specimen welded in the flat position, as previously reported by Evans (Ref. 16), could be related to the fact that in uphill welding the alloying elements' recovery rate is probably different than in the flat position, thus affecting the deoxidation process of the weld metal. This increase in alloying elements results in changes in the austenite decomposition kinetics promoting lower transformation temperature products formation, like AF and FS, and a reduction in PF(G).

The higher amount of PF(G) found in the coupons welded under CO_2 (Fig. 3B) may be related to the corresponding higher oxygen content in the weld metal that would preclude the intragranular nucleation of AF (Refs. 24, 25).

In all welds performed in the uphill position, PF(G) practically disappeared, as shown, for example, in Fig. 3C (A2V) and 3D (C3V).

No important variations in PF(I) and FS(A) were observed with the type of gas shielding or the heat input. When welding under the gas mixture, AF increased and FS(NA) decreased — Fig. 3C, D.

With low heat input (three passes per layer), AF decreased and FS(NA) increased, while the opposite effect was found for high heat input (two passes per layer).

Table 4 also shows the average columnar grain widths, which were measured only in deposits obtained for the flat welding positions for both gas protections, due to the very low amount of PF(G) in welds carried out in the uphill position. It can be seen, as previously found (Refs. 10, 11, 21–23), that the prior austenite grain boundary ferrite size increased as the heat input increased.

Although AF content is also a function of heat input and composition, the large difference in O content, shown by the two point groupings in Fig. 4, was due to the use of different shielding gases, higher O level corresponding to CO_2 shielding and lower O content to the gas mixture. A good relationship between oxygen contents and percentages of AF can be observed: as O content decreased, AF increased, in agreement with the literature (Ref. 26).

Reheated Zones (HAZ)

It was not possible to measure the fine grain size of the low-temperature reheated zone due to the fact that the well-defined equiaxed nature of the plain C-Mn system (Ref. 27) was progressively modified as the ferrite grains were re-

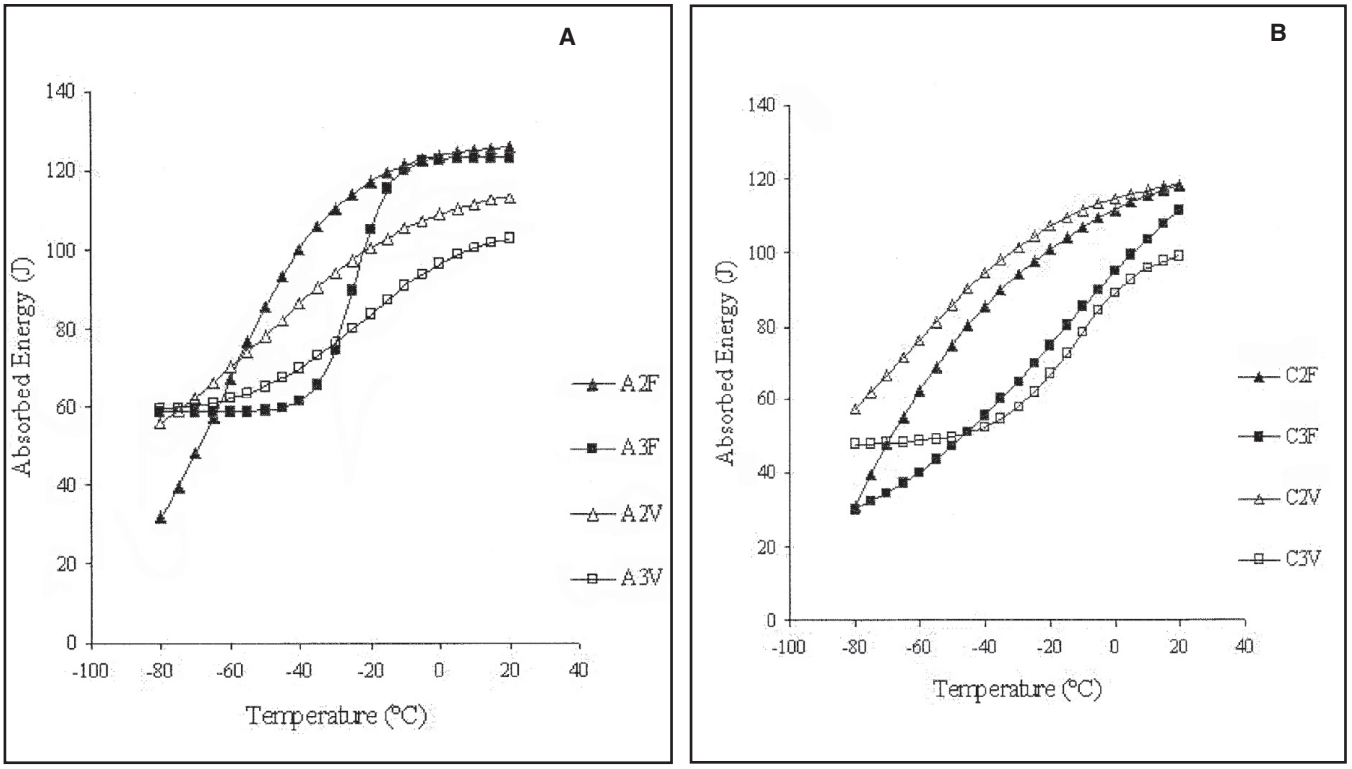

Fig. 6 — Charpy V-notch impact test results. A — Ar/CO_2 shielding gas; B — CO_2 shielding gas (records in Table 6).

Table 7 — Charpy-V Test Temperatures for 50 J of Absorbed Energy

Samples	50 J. T(°C)
C2F	–69
C3F	–47
A2F	–69
A3F	<–80*
C2V	<–80*
C3V	–49
A2V	<–80*
A3V	<–80*

*For the lowest tested temperature (–80°C), the absorbed energy was above 50 J.

Table 8 — Charpy-V Absorbed Energy in J at –51°C (AWS Test Temperature Requirement)

T	–51°C
C2F	74
C3F	47
A2F	83
A3F	59
C2V	85
C3V	50
A2V	77
A3V	65
AWS req.	27 J min

placed by colonies of ferrite of second phase, as previously found by Evans (Ref. 28). This effect can be seen in Fig. 5.

Mechanical Properties

Hardness

Table 3 also presents the microhardness average values. As a general tendency, deposits welded under Ar/CO_2 shielding presented higher average hardness values than those under CO_2 protection, and also the specimens welded in the uphill position compared to those obtained in the flat. In both cases, the increase in hardness was found related to a higher content of alloying elements. This would lead to an increase in hardenability and to solid solution hardening effects.

In general, the average hardness values found in all samples welded with lower heat input (three passes per layer), were higher than those obtained with higher heat input (two passes per layer), as expected (Ref. 12).

Tensile Properties

Table 5 shows tensile test results. In accordance with the results of both chemical composition and hardness measurements, tensile and yield strengths of deposits welded under Ar/CO_2 were higher than those obtained under CO_2 shielding. There was not an important effect of the heat input on tensile strength. In general, yield strength increased with a reduction in heat input in agreement with what was observed for hardness. In all cases, tensile and yield strengths were higher in the uphill welding position.

When welding under Ar/CO_2, with three passes per layer (lower heat input), the tensile E91T5-K2 classification requirements were satisfied but not the E101T5-K3 ones. Elongation values were high, exceeding in all cases the requirements of both AWS classifications.

Charpy-V Impact Properties

The values of absorbed energy for each test temperature in the Charpy-V tests are presented in Table 6, while Fig. 6A and B show the absorbed energy vs. testing temperature for the Charpy-V impact test for different conditions.

Considering the overall toughness results throughout the entire testing temperature range, the best impact behavior was found in samples welded in the uphill position that exhibited flat Charpy curves with high values of absorbed energy, particularly at low temperatures. This effect of welding position may be attributed to the virtual disappearance of grain boundary primary ferrite in the weld metal of the

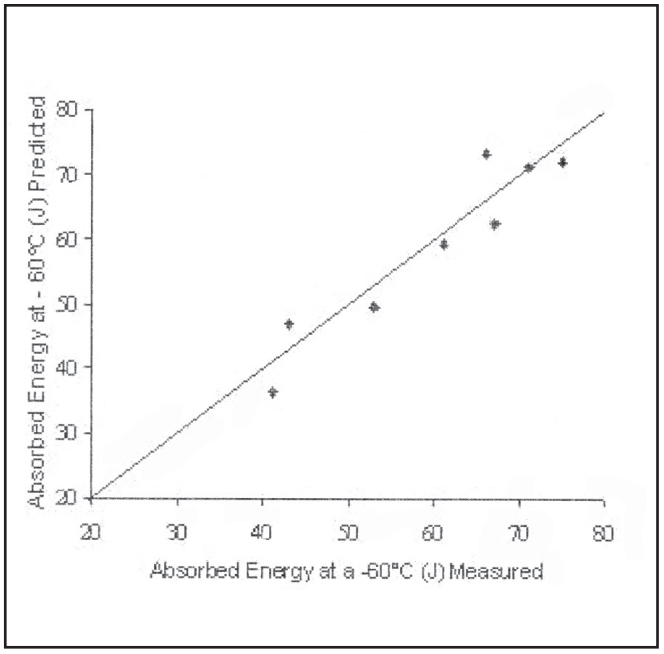

Fig. 7 — Predicted and measured value comparison of absorbed energy at –60°C in Charpy V-notch impact test.

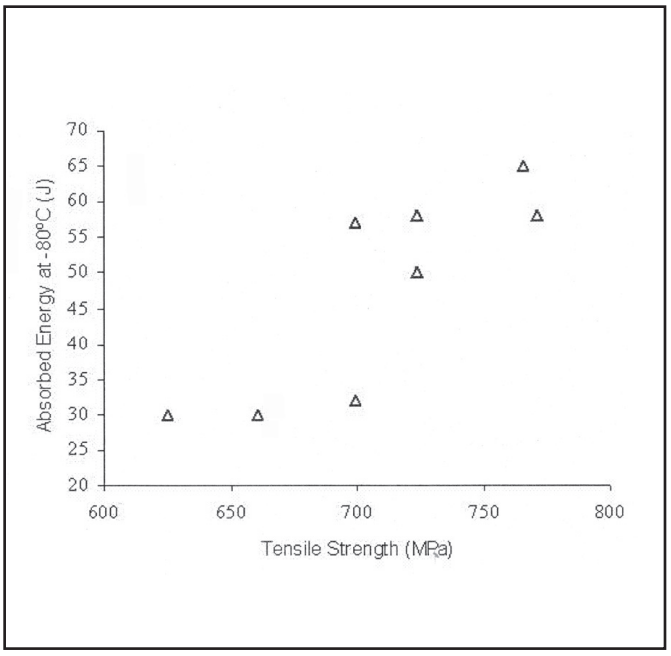

Fig. 8 — Relationship between tensile strength and absorbed energy values at –80°C.

uphill welds and to an increase in both AF and FS(NA) volume fractions. These constituents have high hardness and toughness, with the presence of AF particularly becoming relevant in this respect, as reported in the literature (Refs. 29, 30). This marked reduction in grain boundary primary ferrite can be related to the higher C, Mn, and Si contents found in these welds leading to an increased hardenability of the weld metal. In spite of having found differences in the toughness values for the different welding conditions, the consumable object of this work presented excellent impact properties for the entire temperature range considered and for all the conditions studied. In general, welds produced under the gas mixture presented higher impact values than the corresponding welds made under CO_2 shielding, probably due to higher levels of C, Mn, and Si, and lower O found in the weld metal of the Ar-CO_2 welds. Taking into account values shown in Table 7, it can be seen that all the samples welded under mixture gas shielding absorbed at –80°C (the lowest test temperature used in this work) higher energy than 50 J.

Due to the fact that the best impact results at –51°C (AWS impact test temperature requirement) (Table 8) were achieved with the A2F, C2V, C2F, and A2V samples, no important effects of the type of gas shielding or the welding position were found at this temperature. On the other hand, an influence of the heat input through the number of passes per layer could be detected since the best impact values were obtained with higher heat input (2 passes per layer). This observation may be related to the lower proportion of columnar zone and to a higher amount of acicular ferrite in the weld metal produced with two passes per layer. It can be seen that for any welding condition, the ANSI/AWS A5.29-98 E91T5-K2 and E101T5-K3 requirement of 27 J on average for this temperature was comfortably satisfied, not having presented a single value under the required minimum.

Presenting a Model

The variations in the different welding process parameters studied simultaneously affect the microstructural development in different ways. This is finally reflected on the measured properties of the weld metal that are the resultant of the interaction of those effects (Refs. 16, 21–23, 26). Because of this complex interaction, the consideration of an isolated parameter is generally not effective for the prediction of the final weld metal properties so that an integrated analysis should be undertaken given proper consideration to all the relevant effects and their interaction.

Several factors were thus considered to identify a controlling parameter for toughness that incorporates weld metal chemical composition, proportion of primary and secondary (coarse and fine) zones, fractions of microconstituents measured in the columnar region of the last bead, and grain size.

Thus, a model intended to rationalize the different intervening microstructural factors at the notch location was developed. Two independent expressions were obtained for welds made in the flat and in the uphill positions, since different behaviors were found in each case. Figure 7 shows the result of the application of such a model to estimate the weld metal toughness tested at –60°C, and a comparison between predicted and actually measured values is presented. A good correlation was obtained and the markedly different behaviors between weld metal produced in the flat and in the uphill welding positions are apparent.

The expressions of the model are given by Equation 1 for the flat position and by Equation 2 for the uphill position. These expressions were developed empirically fitting the measured values with the guidance of physical criteria

$$E(-60°C)_F = 0.01\%Col\,[-61 + 0.9\%AF - 0.9\%PF(G) - 0.1ACGW + \%FS(NA)] + 0.15\%FG + 68 \quad (1)$$

$$E(-60°C)_{VUP} = 0.01\%Col\,[-66 + 1.9\%AF + 0.6\%FS(NA)] + 0.3\%FG + 70\,[1.7 - Mn(wt\text{-}\%)] + 28HI + 2 \quad (2)$$

where E stands for Charpy-V absorbed energy, F for flat position, VUP for uphill welding; %Col is the percentage of the columnar zone, ACGW refers to average columnar grain width, %FG is the percentage of fine grain zone, and HI stands for heat input in kJ/mm.

In Fig. 8, the relationship between tensile strength (Table 5) and absorbed energy values at –80°C (Table 6) is shown. An abrupt increase in absorbed energy could be seen for tensile strength values above 700 MPa for the uphill welds.

It can be observed in Fig. 8 that, in some cases, an optimum combination of tensile strength and toughness was obtained with tensile strength in the range of 700–800 MPa and toughness in the range of 50–65 J at –80°C. In these cases, a lower amount of PF(G) was detected together with a higher fraction of AF in the columnar zone. It is well known that a reduction in PF(G) and an increase in AF leads to an improvement in tensile strength and toughness (Refs. 29, 30). In particular, this effect was found in all uphill welds.

Final Remarks

The results obtained in this work showed that, as in the case of SMAW electrodes of the ANSI/AWS A5.5-96 E10018/11018/12018-M types, depositing C-Mn-Ni-Mo or C-Mn-Ni-Mo-Cr alloyed ferritic weld metal (Refs. 10, 11, 31–34), the main difficulty resides in obtaining adequate tensile strength values rather than in satisfying toughness requirements that can be obtained almost in any welding condition, within the requirements of the appropriate standard.

Conclusions

In C-Mn-Ni-Mo ferritic all-weld-metal produced with 1.2-mm-diameter E91T5-K2/101T5-K3 metal cored electrodes, under CO_2 and Ar/CO_2 shielding, in the flat and uphill welding positions, with high arc energy (two passes per layer) and low arc energy (three passes per layer), it was found that

- The all-weld metal from test specimens welded under CO_2 presented lower levels of C, Mn, and Si and higher oxygen contents. Carbon, Mn, and Si were also lower in the flat welding position for both shielding gases and N contents were all very low.
- As a general trend, for both shielding gases, on Charpy V-notch locations, columnar zone percentages were higher for lower heat input (three passes per layer) and the uphill welding position.
- Only in the columnar zones of the samples welded in the flat welding position was it possible to perform the average columnar grain width measurement due to PF(G) being practically absent in the welds performed in the uphill position.
- In the columnar zones of welds made under CO_2, AF volume fraction was lower and PF(G) volume fraction was higher than in those made under Ar/CO_2.
- Hardness measured in the specimens welded under CO_2 was lower than that in specimens made using the Ar/CO_2 mixture. A similar effect was found with higher heat input (two passes per layer) when compared to specimens with lower heat input (three passes per layer).
- The tensile properties were higher in welds made under the Ar/CO_2 mixture and with three passes per layer, in correlation to chemical composition and hardness results.
- Impact properties were excellent in all the conditions studied. The best results were obtained under the Ar/CO_2 mixture shielding, up to –40°C. It was not possible to find a behavior pattern with the parameter variation used.
- With CO_2 shielding, best toughness was obtained in the uphill welding position and with two passes per layer, if all the test temperature range is considered.
- ANSI/AWS A5.29-98 E91T5-K2M tensile property requirements were satisfied under Ar/CO_2, E91T5-K2/K2M and E101T5-K3/K3M impact requirements were very comfortably satisfied in all the welding conditions, and the all-weld-metal chemical composition met the E101T5-K3/K3M requirement.

Acknowledgments

The authors wish to express their gratitude to Air Liquide Argentina S.A. for supplying the consumables and the facilities for the production of the welds; to the Centre Téchnique des Applications du Soudage, Air Liquide France, for conducting nitrogen and oxygen determinations and for useful discussions; to Siderca, Argentina, for oxygen and nitrogen determinations; to Conarco-ESAB Argentina for carrying out the chemical analyses; and to the Fundación Latinoamericana de Soldadura, Argentina, for the facilities provided to weld and for machining and mechanical testing. The authors recognize ANPCyT, Argentina, for its financial support.

References

1. Myazaki, T. 1988. Flux cored wires for robots. Hitachi Zosen Corp. Ariabe Works, *IIW-IIS Doc XII-1084-88*.

2. Ferree, S. E. 1995. New generation of cored wires creates less fume and spatter. *Welding Journal* (74)12: 45–49.

3. Sakai, Y., Aida, G., Suga, T., and Nakano, T. 1989. Development of various flux-cored wires and their application in Japan. *IIW/IIS Doc. XII-1131-89.*

4. Sakai, Y., Aida, G., Suga, T., and Nakano, T. 1989. Metal type flux-cored wire for carbon steel. *IIW/IIS Doc. XII-1131-89.*

5. Lathhabai, S., and Stout, R. D. 1985. Shielding gas and heat input effects on flux cored weld metal properties. *Welding Journal* 64(11): 303-s to 313-s.

6. Myers, D. 2002. Metal cored wires: Advantages and disadvantages. *Welding Journal* 81(9): 39–42.

7. Huisman, M. D. 1996. Flux and metal-cored wires, a productive alternative to stick electrodes and solid wires. *Svetsaren* 51, No. 1–2, 6–14.

8. Lyttle, K. 1996. Metal cored wires: Where do they fit in your future? *Welding Journal* 75(10): 35–38.

9. Schumann, G. O., and French, I. E. 1995. The influence of welding variables on weld metal mechanical and microstructural properties from conventional and microalloyed rutile flux-cored wires. *Australian Welding Research.* CRC No. 8, June, pp. 1–12.

10. Vercesi, J., and Surian, E. 1996. The effect of welding parameters on high-strength SMAW all weld metal — Part 1: AWS E11018M. IIS-IIW Doc II-A-915-94. *Welding Journal* 75(6): 191-s to 196-s.

11. Vercesi, J., and Surian, E. 1997. The effect of welding parameters on high-strength SMAW all-weld-metal — Part 2: AWS E10018M and E12018M. IIW-IIS Doc II-A-934-94. *Welding Journal* 77(4): 164-s to 171-s.

12. Gianetto, J. A., Smith, N. J., McGrath, J. T., and Bowker, J. T. 1992. Effect of composition and energy input on structure and properties of high-strength weld metals. *Welding Journal* 71(11): 407-s to 419-s.

13. Strunck, S. S., and Stout, R. D. 1972. Heat treatment effects in multi-pass weldments of a high-strength steel. *Welding Journal* 51(10): 508-s to 520-s.

14. Glover, A. G., McGrath, J. T., Tinkler, M. J., and Weatherly, G. C. 1997. The influence of cooling rate and composition on weld metal microstructures in a C/Mn and a HSLA steel. *Welding Journal* 56(9): 267-s to 273-s.

15. Dorschu, K. E. 1968. Control of cooling rates in steel weld metal. *Welding Journal* 47(2): 49-s to 62-s.

16. Evans, G. M. Effect of welding position on the microstructure and properties of C-Mn all-weld metal deposits. *Welding Review,* 1982, 1(3): 6–10. *Welding Res. Abroad*, 1983, 29(1): 46–7.

17. Vaidya, V. 2002. Shielding gas mixtures for semiautomatic welds. *Welding Journal* 81(9): 43–48.

18. ANSI/AWS A5.29-98, *Specification for Low-Alloy Steel Electrodes for Flux Cored Arc Welding*. 1998. Miami, Fla.: American Welding Society.

19. Schnadt, H. M., and Leinhard, E. W. 1963. Experimental investigation of the sharp-notch behavior of 60 steels at different temperature and strain rates. *IIW-IIS Doc. 196-343-63.*

20. Guide to the light microscope examina-

tion of ferrite steel weld metals. *IIW Doc. IX-1533-88*.

21. Ramini de Rissone, N. M., de Souza Bott, I., de Vedia, A., and Surian, E. 2003. The effect of welding procedure ANSI/AWS A5.20-95 E71T1 flux cored wire deposits. *STWJ* 8(2): 113–122.

22. Svoboda, H. G., Ramini de Rissone, N. M., de Vedia, L. A., and Surian, E. 2003. The effect of welding procedure on ANSI/AWS A5.29-98 E81T1-Ni1 flux cored wire deposits. *IIW-IIS Doc. II-A-0136-04*. *Welding Journal*, 2004, 83(11): 301-s to 307-s.

23. Evans, G.M. 1982. Effect of heat input on the microstructure and properties of C-Mn all-weld-metal deposits. *Welding Journal* 61(4): 125-s to 132-s. *Welding Research Abroad,* 1983, 29(1): 35; *IIW Doc IIA-490-79.*

24. Ferrante, M., and Farrar, R. A. 1982. The role of oxygen rich inclusions in determining the microstructure of weld metal deposits. *Journal of Materials Science* 17: 3293–3298.

25. Babu, S. S., David, S. A., Vitek, J. M., Mundra, K., and DebRoy, T. 1995. Development of macro- and microstructures of carbon-manganese low alloy steel welds: Inclusion formation. *Material Science and Technology* 11: 186–199.

26. Francis, R. E., Jones, J. E., and Olson, D. L. 1990. Effect of shielding gas oxygen activity on weld metal structure of GMA welded microalloyed HSLA steel. *Welding Journal* 69(11): 408-s to 415-s.

27. Evans, G. M. 1983. Effect of carbon on the microstructure and properties of C-Mn all-weld-metal deposits. *Welding Journal* 62(11): 313-s to 320-s; *Welding Res. Abroad,* 1983, 29(1): 58–70; *IIW Doc II-983-82*.

28. Evans, G. 1991. The effect of nickel on the microstructure and properties of C-Mn all-weld metal deposits. *Joining Sciences* 1(1): 2s–13s; *Welding Research Abroad,* 1991, 37(2/3): 70–83; *IIW Doc. IIA-791-89.*

29. Bhadeshia, H. K. D. H., and Svensson, L. E. 1993. *Mathematical Modelling of Weld Phenomena*. London, U.K.: Institute of Materials.

30. Abson, D. J., and Pargeter, R. J. 1986. Factors influencing as-deposited strength, microstructure and toughness of manual metal arc welds suitable for C-Mn steel fabrications. *International Metals Reviews* 31(4): 141–196.

31. Surian, E., Trotti, J., Cassanelli, A. N., and de Vedia, L. A. 1987. Influence of Mn content on mechanical properties and microstructure of a high strength SMA electrode weld metal. *IIW-IIS Doc. II-A-724-87.*

32. Surian, E., Trotti, J., Herrera, R., and de Vedia, L. A. 1991. Influence of C on mechanical properties and microstructure of weld metal from a high-strength SMA electrode. *Welding Journal* 70(6): 133-s to 140-s.

33. Surian, E., Trotti, J., Cassanelli, A. N., and de Vedia, L. A. 1994. Influence of chromium on mechanical properties and microstructure of weld metal from a high strength SMA electrode. *IIW-IIS Doc. II-1204-92. Welding Journal* 73(3): 45-s to 53-s.

34. Surian, E., Ramini de Rissone, M., and de Vedia, L. 2005. Influence of molybdenum on ferritic high-strength SMAW all-weld-metal properties. *Welding Journal* 84(4): 53-s to 62-s.

CAN WE TALK?

The *Welding Journal* staff encourages an exchange of ideas with you, our readers. If you'd like to ask a question, share an idea or voice an opinion, you can call, write, e-mail or fax. Staff e-mail addresses are listed below, along with a guide to help you interact with the right person.

Publisher/Editor
Andrew Cullison
cullison@aws.org, Ext. 249
Article Submissions

Senior Editor
Mary Ruth Johnsen
mjohnsen@aws.org, Ext. 238
Feature Articles

Associate Editor
Howard Woodward
woodward@aws.org, Ext. 244
New Literarure, Society News
Personnel, Coming Events

Assistant Editor
Kristin Campbell
kcampbell@aws.org, Ext. 257
New Products
News of the Industry
Press Time News

Production Editor
Zaida Chavez
zaida@aws.org, Ext. 265
Design and Production

Advertising Sales Director
Rob Saltzstein
salty@aws.org, Ext. 243
Advertising Sales

Advertising Production Coordinator
Frank Wilson
fwilson@aws.org, Ext. 465
Advertising Production

Advertising Sales & Promotion Coordinator
Lea Garrigan
garrigan@aws.org, Ext. 220
Production and Promotion

Peer Review Coordinator
Doreen Kubish
doreen@aws.org, Ext. 275
Peer Review of Research Papers

Welding Journal Dept.
550 N.W. LeJeune Rd.
Miami, FL 33126
(800)/305 443-9353
FAX (305) 443-7404